2007

Ferromagnetic to ferrimagnetic crossover in Cr-doped GaN nanohole arrays

Q. Wang
Virginia Commonwealth University

Q. Sun
Virginia Commonwealth University

Puru Jena
Virginia Commonwealth University, pjena@vcu.edu

Y. Kawazoe
Tohoku University

Wang, Q., Sun, Q., Jena, P., et al. Ferromagnetic to ferrimagnetic crossover in Cr-doped GaN nanohole arrays. Physical Review B, 75, 075312 (2007).

Ferromagnetic to ferrimagnetic crossover in Cr-doped GaN nanohole arrays

Q. Wang, Q. Sun, and P. Jena
Department of Physics, Virginia Commonwealth University, Richmond, Virginia 23284-2000, USA

Y. Kawazoe
Institute for Materials Research, Tohoku University, Sendai 980-8577, Japan

(Received 21 July 2006; revised manuscript received 22 December 2006; published 9 February 2007)

Using spin-polarized density-functional theory with exchange and correlation potential, approximated by both the generalized gradient approximation (GGA) and the GGA+U methods, we show that the coupling between a pair of Cr atoms substituted in GaN nanoholes is ferromagnetic. The interaction between the two Cr atoms, each carrying an average magnetic moment of around $2.5\mu_B$, is short ranged and mediated by the neighboring N atom. As the concentration of Cr increases, clustering ensues and the coupling changes from ferromagnetic to ferrimagnetic resulting in a significant reduction in the average magnetic moment per Cr atom.

DOI: 10.1103/PhysRevB.75.075312 PACS number(s): 75.50.Pp, 36.40.Cg, 75.30.Kz, 75.75.+a

I. INTRODUCTION

The discovery of extraordinary optical transmission of subwavelength hole arrays[1] has led to intensive research on periodic metal nanohole (NH) arrays (ordered nanoporous materials),[2–10] which, compared to their bulk counterparts, exhibit many unique properties with potential technological applications in nanophotonic devices,[3–5] information storage,[6,7] solar cells,[8] near-field scanning optical microscopy,[6] surface-enhanced Raman spectroscopy[9] and biosensors.[10] Recently, increasing interest is being focused on nanoporous wide band-gap semiconductors such as GaN nanopore arrays,[11–16] primarily due to their high thermal, chemical, and mechanical stability and their potential applications in optoelectronics, chemical, and biochemical sensing. For example, high optical quality nanoporous GaN has been synthesized[14,15] and the fascinating luminescence properties of nanoporous GaN films have been reported.[16] However, the use of GaN NH arrays as a template for doping transition-metal atoms has not yet been explored. This is particularly interesting as such systems may result in ferromagnetic (FM) coupling between transition-metal atoms and hence have the potential for applications in spintronics devices.

In this paper we report state-of-the-art first-principles calculations of Cr-doped GaN NH arrays and demonstrate their magnetic properties and potential for new applications in spintronics. Earlier studies have shown that Mn doped GaN thin film is anti-ferromagnetic (AFM),[17] while Mn-doped GaN nanowires (NWs) are FM due to the confinement of electrons in the radial direction and the curvature of the NWs.[18] The common feature of NWs and NHs is that both are characterized by curved surfaces, which affect the interatomic distances as well as the orbital interactions between the doped transition-metal atoms. However, the doped transition-metal atoms would reside on the concave side of the surface while in NWs they reside on the convex side of the surface. Since the magnetic coupling between transition-metal atoms in GaN is sensitive to the interatomic distance, it is of interest to know if the coupling in NH arrays remains ferromagnetic as in NWs. Here we concentrate on the Cr atom. Because of its unique electronic configuration of [Ar] $3d^5 4s^1$ and the small energy gap between the $3d$ and $4s$ orbitals, Cr can exist in different oxidation states, namely, 0, +2, +3, and +6, which can be used to tune the structure and magnetic properties of a Cr-doped material. Our objectives are (i) to calculate the preferred sites of Cr atoms—whether they occupy the interior surface sites, or penetrate into the bulk; (ii) to predict the magnetic coupling between Cr atoms in the NH arrays, and (iii) to determine if Cr atoms prefer to cluster as their concentration grows and how the magnetic coupling between them depends on their interatomic distance.

II. THEORETICAL APPROACH

The GaN NH has been generated from a $(5\times5\times2)$ GaN supercell having wurtzite crystal structure and experimental lattice consists (a=3.189 Å, c=5.185 Å). We removed Ga and N atoms from a hexagonal unit along the [0001] direction and replaced it with a vacuum space, thus creating a NH supercell (see Fig. 1), which contains 88 Ga atoms and 88 N atoms. Periodic repetition of the supercell along the $[10\bar{1}0]$, $[01\bar{1}0]$, and [0001] directions yields the NH arrays (see Fig. 2). This NH has a polygon periphery with the diameters of 7.81 Å for the inner layer and 9.76 Å for the outer layer of the hole when viewed from the central axis of the NH along the [0001] direction.

To study the magnetic coupling between Cr atoms in the NH, we have replaced a pair of Ga atoms with Cr atoms at different sites to simulate the Cr-doped GaN NH. This replacement corresponds to a 2.27%-Cr doping concentration and results in the $Ga_{86}Cr_2N_{88}$ NH supercell. There are many ways to model this substitution, depending upon the sites where Cr atoms are distributed. It has been well established that Cr atoms prefer to cluster around neighboring N and reside on the outermost surface layer in the Cr-doped GaN thin film[19] and the Cr-doped GaN NWs.[20] In this study we have generated five configurations to study the preferred sites of Cr. These are specified in Table I. The total energies

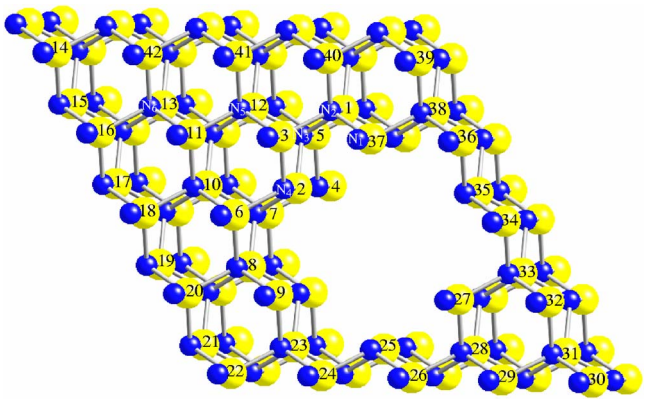

FIG. 1. (Color online) Schematic representation of a GaN NH ($Ga_{88}N_{88}$) supercell. The lighter (yellow) and numbered spheres are Ga, and the darker (blue) and smaller spheres are N. In the supercell the directions through atoms 22 and 24, 22, and 20, and 4 and 2 correspond to, $[10\bar{1}0]$, $[01\bar{1}0]$, and [0001], respectively.

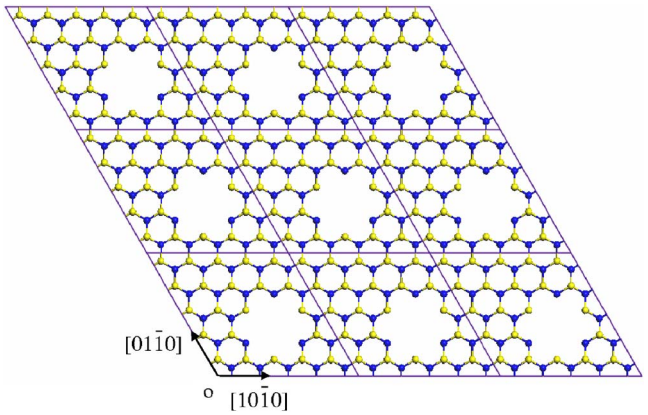

FIG. 2. (Color online) Top view of $3\times3\times3$ GaN NH supercells which extends to infinite length along the [0001] direction.

corresponding to both FM and AFM spin alignments for all the configurations were calculated to determine the preferred geometric and magnetic ground state. To explore the magnetic interaction between Cr atoms and the effect of Cr concentration on the magnetic coupling, we have also performed the calculations where three and four Ga atoms have been separately replaced with Cr atoms in the supercell. All possible spin couplings between these atoms were considered. From the total energies we calculated the preferred magnetic coupling as well as the magnetic moments located at each Cr atom self-consistently.

The electronic and magnetic properties have been computed using the spin-polarized density-functional theory (DFT) and different levels of correlation corrections [generalized gradient approximation (GGA) and GGA+U] which are implemented in Vienna *Ab initio* Simulation Package (VASP).[21] We used a plane-wave basis set and the projector augmented wave (PAW) potentials[22,23] for Ga, N, and Cr atoms and PW91 form[24] for the generalized gradient approximation (GGA) for the exchange and correction potentials. To study the effect of Coulomb correlation on the electronic structure and magnetic coupling of the Cr-doped GaN NH, we have also employed the GGA+U method[25,26] and considered the Coulomb correction $U=3$ eV and the exchange interaction parameter $J=0.87$ eV for Cr $3d$ electrons, which have been used in previous calculations.[27,28] The k-points convergence was achieved with $(3\times3\times4)$ Monkhorst-Pack grid,[29] and tests with up to $(4\times4\times5)$ k-points mesh were performed. The energy cutoff for plane waves in all the calculations was set at 330 eV, where the convergence in energy and force was set to 10^{-4} eV and 10^{-3} eV/Å, respectively.

III. RESULTS AND DISCUSSIONS

The properties of Cr-doped GaN NH arrays are discussed in succeeding steps. We begin this work by looking at the electronic structure of the pure GaN NH. The total-energy calculation and geometry optimization were carried out by allowing the atomic coordinates of all the atoms in the NH supercell relax without any symmetry constraint. It was found that the relaxed bond length of Ga-N dimer on the outer layer (such as Ga_1-N_2, Ga_5-N_3) and inner layer (such as Ga_{37}-N_1, Ga_2-N_4) of the NH along the [0001] direction is 1.846 and 1.957 Å, corresponding to a contraction of −6.09% and −1.46% from the bulk value, respectively. The bond length of Ga-N dimers, where the Ga and N are in the same (0001) plane of the NH surface (such as Ga_3-N_2 and Ga_{37}-N_2), changes from 1.939 to 1.926 Å. For the bulk sites, on the other hand, the Ga-N bond length (such as Ga_{11}-N_5 and Ga_{11}-N_6) is 1.953 Å corresponding to a small expansion of 0.73%, and that for the atoms along the [0001] direction

TABLE I. The energy difference ΔE between AFM and FM states (eV), the relative energy $\Delta\varepsilon$ (eV) calculated with respect to ground-state configuration I (configuration II), and the optimized Cr-Cr and the nearest Cr-N distances (Å) for the $Ga_{86}Cr_2N_{88}$ NH supercell using GGA (GGA+U).

	ΔE (coupling)		$\Delta\varepsilon$		$d_{\text{Cr-Cr}}$		$d_{\text{Cr-N}}$	
Configurations	(GGA)	(GGA+U)	(GGA)	(GGA+U)	(GGA)	(GGA+U)	(GGA)	(GGA+U)
I(1, 2)	0.128	0.115	0.000	0.054	3.102	3.117	1.797	1.871
II(3, 2)	0.182	0.235	0.015	0.000	3.032	3.086	1.801	1.831
III(2, 9)	−0.084	−0.022	0.202	0.237	5.386	5.310	1.788	1.851
IV(3, 11)	0.147	0.126	0.930	1.072	3.108	3.133	1.820	1.866
V(11, 12)	0.192	0.163	0.958	1.142	3.075	3.087	1.890	1.913

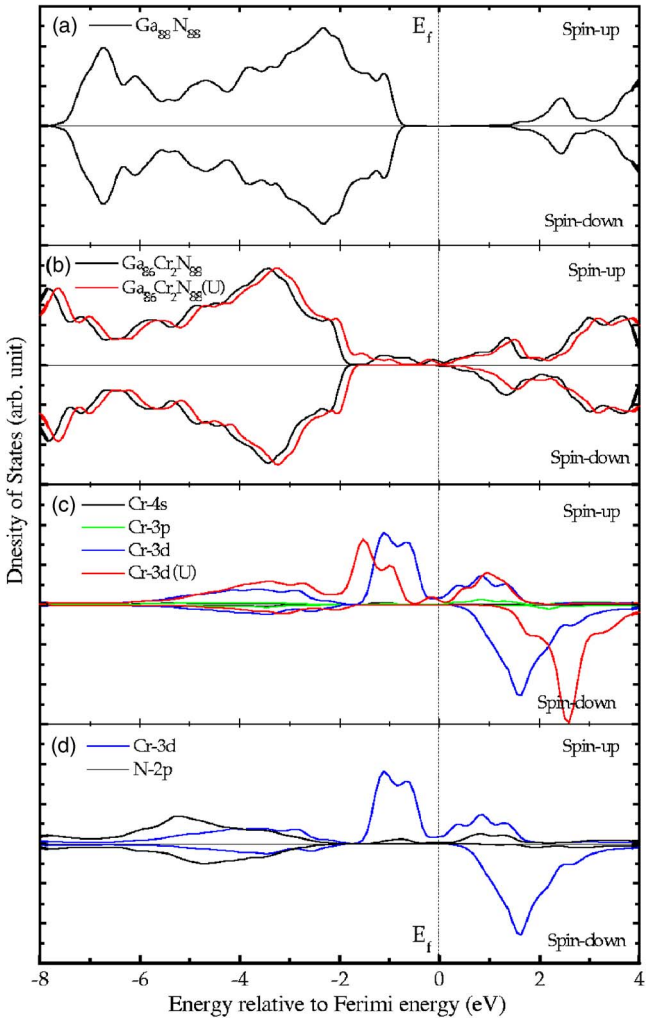

FIG. 3. (Color online) (a) Total DOS corresponding to pure $Ga_{88}N_{88}$ NH, (b) total DOS of Cr-doped GaN-NH, (c) partial spin DOS of Cr atom, and (d) partial spin DOS of Cr 3*d* and N 2*p* in $Ga_{86}Cr_2N_{88}$ supercell.

(such as Ga_{13}-N_6, Ga_{12}-N_5) changes from 1.986 to 1.962 Å. The total energy of the relaxed supercell was found to be 5.685 eV lower than that for the unrelaxed one. Assuming that this energy gain is shared by the atoms on the NH surface that have relaxed the most, it was found that the energy gain per surface Ga-N dimer is 0.164 eV, which is slightly larger than that in GaN surface.[19] The total electronic density of states (DOS) for spin-up and spin-down electrons corresponding to the pure NH supercell is plotted in Fig. 3(a), which is characterized by a large gap. The Fermi level is located in the gap region and the spin-up and spin-down DOS are totally symmetric, therefore the pure GaN NH still retains the wide gap semiconductor feature of GaN bulk.

We next discuss the magnetic coupling between two Cr atoms in the NH. We have replaced a pair of Ga atoms with Cr at different sites and have chosen five configurations. The main results are summarized in Tables I and II. In the first column of Table I, we specified the five configurations by giving the sites where the Ga atoms have been replaced with Cr. Configuration I and configuration II correspond to the substitutions of a pair of Ga atoms with Cr at the nearest-neighbor sites (1, 2) and (3, 2) on the NH surface (see Fig. 1), respectively. Configuration III relates to the replacement of Ga atoms at the next nearest sites (2, 9). This was done to verify if clustering of Cr atoms seen in GaN bulk, thin film, and NWs still persists in the NH. To study the effect of the curvature of the NH on the site preference of Cr atoms, we created configurations IV and V. The former corresponds, respectively, to replacing one Ga at surface site 3 and another one at nearest bulk site 11, while in the latter Ga atoms at bulk sites (11, 12) forming the nearest neighbor were replaced with Cr atoms. Total-energy calculations with full geometry optimizations have been performed for both FM and AFM spin alignments for all the five configurations. The energy difference ΔE between the AFM and FM states $[\Delta E = E(\mathrm{AFM}) - E(\mathrm{FM})]$ related to the relaxed configurations are listed in the second column of Table I, which indicates the preferred magnetic coupling between the two Cr atoms. Configuration I was found to be the ground state with the FM state lying 0.128 eV lower in energy than the AFM state. Using the total energy of the ground state as reference, the relative energies $\Delta\varepsilon$ calculated with respect to the other four configurations are given in Table I. Comparing the relative energies in the fourth column, we note that the Cr atoms prefer to occupy the surface sites of the NH, cluster around nearest N atoms, and couple ferromagnetically, as was found in Cr-doped GaN thin films[19] and NWs. The configurations with the Cr atoms at the bulk sites (configuration IV and V) are found to be higher in energy by 0.958 and 0.910 eV than the ground state, respectively. Configuration III with the two Cr atoms residing in the next-nearest surface sites is also found to be higher in energy by 0.20 eV than the ground-state configurations. Configurations I and II are energetically nearly degenerate with the latter one being 0.015 eV higher in energy. The optimized geometries of these configurations retain the same structural feature as the initial polygonal hole. In the ground-state configuration, the calculated Cr-N bond length is 1.899 and 1.905 Å for Cr_1-N_3 and Cr_2-N_3, respectively (see Fig. 1) and the shortest distance between Cr and N is that for Cr_1-N_2, namely 1.797 Å, along the [0001] direction, which contracted by −2.7%, as compared to that in the pure NH. We tabulated the distances between the two Cr atoms and that between the Cr and N in the nearest-neighbor position in Table I.

The total DOS corresponding to the ground state is shown in Fig. 3(b). The partial DOS for the Cr atom and the partial DOS for the Cr 3*d* and the nearest N 2*p* states are plotted in Figs. 3(c) and 3(d), respectively. It is clear that the energy gap has disappeared and the Cr 3*d* majority states dominate the total DOS in the band-gap region. The DOS for spin up and spin down is no longer identical and the Fermi energy passes through the spin-up DOS and through the gap in spin-down DOS [see Fig. 3(b)]. This system therefore is half metallic. There is a visible overlap between Cr 3*d* and N 2*p* states [see Fig. 3(d)] and the majority N 2*p* states are more hybridized with Cr 3*d* orbitals than the minority states. One can expect that the exchange interaction between the two Cr atoms is mediated by the N 2*p* orbitals. The two Cr atoms are 3.1 Å from each other and the N atom between them forms an angle of about ∠Cr-N-Cr=109°. The three unpaired electrons of N 2*p* orbitals delocalize and overlap with

TABLE II. Local magnetic moments (in μ_B) at each Cr atom and its nearest-neighbor N for each configuration at the GGA and GGA +U level of calculations.

		μ_{total}	μ_s	μ_p	μ_d	μ_{total}	μ_s	μ_p	μ_d
Configurations		(GGA)				(GGA+U)			
I	Cr_1	2.786	0.056	0.017	2.713	3.076	0.048	0.011	3.076
	Cr_2	2.129	0.015	0.028	2.085	2.629	0.020	0.032	2.577
	N	−0.166	−0.005	−0.161		−0.136	−0.007	−0.129	
II	Cr_1	2.978	0.052	0.028	2.898	3.257	0.047	0.023	3.188
	Cr_2	2.263	0.014	0.031	2.218	2.570	0.017	0.025	2.528
	N	−0.092	−0.005	−0.087		−0.243	−0.006	−0.237	
III	Cr_1	2.700	0.053	0.009	2.700	2.941	0.047	0.002	2.891
	Cr_2	−2.028	−0.012	−0.021	−1.995	−2.673	−0.019	−0.035	−2.619
	N	0.058	−0.006	0.064		0.107	−0.002	0.109	
IV	Cr_1	2.273	0.016	0.044	2.213	2.798	0.035	0.008	2.755
	Cr_2	2.448	0.018	0.041	2.390	2.734	0.022	0.019	2.693
	N	−0.095	−0.005	−0.090		−0.141	−0.006	−0.135	
V	Cr_1	2.493	0.019	0.047	2.428	2.773	0.027	0.047	2.626
	Cr_2	2.493	0.019	0.047	2.428	2.790	0.025	0.047	2.625
	N	−0.104	−0.006	−0.099		−0.126	−0.015	−0.111	

the 3*d* orbitals of both the adjoining Cr sites. Note that they can only delocalize into the orbitals containing an opposite spin electron according to Pauli principle. However, the intra-atomic exchange (Hund's rule) will maintain the parallel alignment of the spins on the 2*p* orbitals for N as well as the spins on the 3*d* orbitals for each Cr atom on both sides. Because the interaction leading to the delocalization is spin independent, the itinerant N 2*p* electrons force the core spins of the Cr sites into parallel alignment, consequently, resulting in the FM coupling of the two Cr atoms. We plotted the charge-density distribution for the pure GaN NH and the Cr-doped NH in Figs. 4(a) and 4(b). They show that there is a strong interaction between the Cr atoms and the neighboring N atom.

The magnetic moments located on each Cr atom have been calculated self-consistently for all the configurations. It

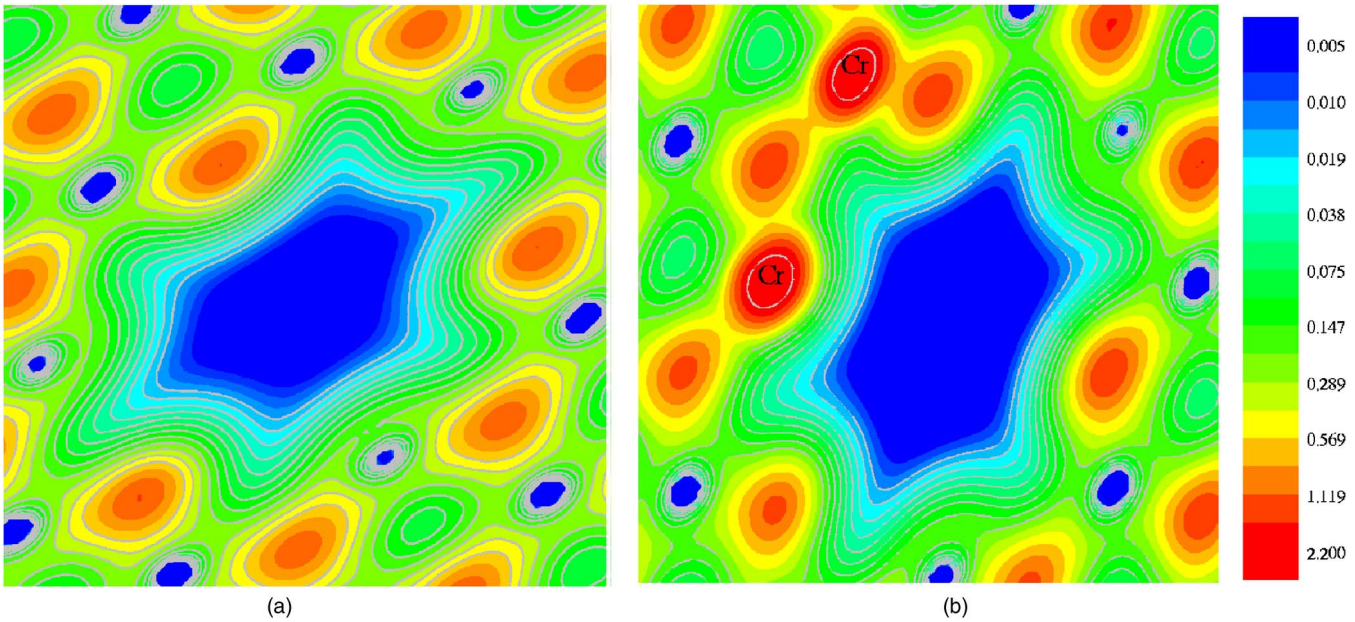

FIG. 4. (Color online) Charge density distribution in (a) $Ga_{88}N_{88}$ and in (b) $Ga_{86}Cr_2N_{88}$ supercells in the plane containing Cr and neighboring N atoms.

was found that, in the ground-state configuration, the magnetic moments located on the Cr_1 and Cr_2 are $2.786\mu_B$ and $2.129\mu_B$, respectively, and mainly arise from the Cr $3d$ orbitals ($2.713\mu_B$ and $2.086\mu_B$, respectively). The partial DOS of Cr in Fig. 3(c) confirms the latter statement. The difference of the local moments on Cr atoms results from the different doping sites. The neighboring N atom is polarized antiferromagnetically and carries a magnetic moment of $-0.166\mu_B$. The magnetic moments at each Cr site and its nearest-neighbor N for all the configurations are given in Table II. It shows that the Cr atoms carry slightly different moments ranging from $2.129\mu_B$ to $2.978\mu_B$ since they occupy different sites in the NH, and they mainly come from the Cr $3d$ orbitals (from $1.995\mu_B$ to $2.898\mu_B$). The neighboring N atoms are polarized antiferromagnetically with the values of the moments ranging from $-0.058\mu_B$ to $-0.166\mu_B$.

To confirm that the calculated ferromagnetism in Cr-doped GaN NH is not a consequence of the approximation to the exchange and correlation potential, we have employed the GGA+U method. This replaces the Coulomb interaction among the localized electrons (e.g., transition metal d) by statically screened parameters U and J. We considered the Coulomb correction for Cr $3d$ electrons in the calculations for all the configurations of the $Ga_{86}Cr_2N_{88}$ supercell and relaxed the geometries for both FM and AFM alignments without any symmetric constraint. The main results are summarized in Tables I and II to facilitate comparison with those from GGA calculations. The total DOS for the ground state and the partial DOS for Cr $3d$ are plotted in Figs. 3(b) and 3(c), respectively. The Coulomb correlation effects are obvious: GGA+U changed the ground-state configuration, namely configuration II is the ground state with FM state lying 0.235 eV lower in energy than AFM, instead of configuration I, and it enhances the gap and the exchange splitting of Cr $3d$ at the Fermi level. As shown in Fig. 3(c), there is a downward shift of the Cr $3d$ spin-up valence states (i.e., the high peak DOS near ~ -1.2 eV shifts down to ~ -1.6 eV from the Fermi energy E_F), and an upward shift of the Cr $3d$ spin-down conduction states from (~ 1.6 to ~ 2.6 eV away from the E_F). But the total DOS at the Fermi level E_F is suppressed in the GGA+U calculation, as shown in Fig. 3(b). GGA+U also gives larger spin and orbital magnetic moments at each Cr atom. The local magnetic moment at the Cr site consequently increased. The moment for configuration II, for instance, reaches the value $3.257\mu_B$ from $2.978\mu_B$ (GGA result), and that for configuration I changes from $2.786\mu_B$ to $3.076\mu_B$. Moreover, it increases the bond lengths between Cr atoms as well as those between Cr and N atoms, see Table I. It is important to note that the introduction of U does not change the magnetic coupling between the Cr atoms, although GGA and GGA+U methods lead to different ground-state configurations. In fact, GGA+U gives a better description of the electronic structure.

To further explore the magnetic interaction between the Cr atoms and the effect of Cr concentration on the magnetic coupling between Cr atoms in the GaN NH system, we have performed additional calculations for the configurations where three and four Ga atoms were replaced by Cr in the supercell, corresponding to a slightly higher Cr concentration of 3.4% and 4.5%, respectively. We have replaced three and four Ga atoms with Cr atoms at different sites, respectively, and have carried out extensive search for their most favorable geometric and magnetic configurations. Four typical configurations, as shown in Fig. 5, have specifically been discussed for the case where three Cr atoms were substituted. These correspond to replacing Ga at sites (3, 2, 6), (3, 6, 9), (3, 2, 8), and (3, 6, 11) with Cr atoms in Fig. 1. For each configuration, calculations were carried out for different spin alignments, namely FM ($\uparrow\uparrow\uparrow$), and ferrimagnetic ($\uparrow\downarrow\uparrow$), ($\uparrow\uparrow\downarrow$), ($\downarrow\uparrow\downarrow$), ($\uparrow\downarrow\downarrow$). It was found that configuration I is energetically most stable lying lower in energy by 0.182, 0.344, and 0.680 eV than the other three configurations, respectively. For the ground-state configuration, it was found that the ($\uparrow\uparrow\downarrow$) spin alignment is lower by 0.051, 0.230, 0.192, and 0.221 eV in energy than that for ($\uparrow\uparrow\uparrow$), ($\uparrow\downarrow\uparrow$), ($\downarrow\uparrow\downarrow$), and ($\uparrow\downarrow\downarrow$), respectively. The total moment for this ground state was found to be $2.775\mu_B$ with each Cr atom carrying a local moment of $(2.274, 2.990, -2.695)\mu_B$. For the case where four Cr atoms were substituted, the total-energy calculations also clearly show that Cr atoms prefer to cluster. The most stable configuration is the one where the four Cr atoms occupy the nearest-neighbors sites (3, 2, 7, 6). This configuration, for instance, is 0.557 eV lower in energy than the configuration where the two dimers of Ga atoms at sites (3, 6) and (5, 7) being 5.19 Å from each other were substituted. For this ground-state configuration, calculations were also carried out for different spin alignments, namely ($\uparrow\uparrow\uparrow\uparrow$), ($\uparrow\downarrow\uparrow\downarrow$), ($\uparrow\downarrow\downarrow\uparrow$), ($\uparrow\uparrow\downarrow\downarrow$), ($\downarrow\uparrow\uparrow\uparrow$), ($\uparrow\downarrow\uparrow\uparrow$), ($\uparrow\uparrow\downarrow\uparrow$), and ($\uparrow\uparrow\uparrow\downarrow$). It was found that the energetically most favorable spin state again is ferrimagnetic ($\downarrow\uparrow\uparrow\uparrow$) with a total magnetic moment of $6.863\mu_B$. The magnetic moment on each Cr atom is $(-1.605, 3.055, 2.484, 2.529)\mu_B$. This spin coupling state, is respectively, 0.088, 0.137, 0.326, 0.259, 0.175, 0.210, and 0.191 eV lower in energy than ($\uparrow\uparrow\uparrow\uparrow$), ($\uparrow\downarrow\uparrow\downarrow$), ($\uparrow\downarrow\downarrow\uparrow$), ($\uparrow\uparrow\downarrow\downarrow$), ($\uparrow\downarrow\uparrow\uparrow$), ($\uparrow\uparrow\downarrow\uparrow$), and ($\uparrow\uparrow\uparrow\downarrow$) configurations. It was found that the FM and AFM states for the configuration where the two Cr pairs are 5.19 Å from each other is energetically nearly degenerate. The results indicates that the Cr atoms indeed prefer to cluster in the GaN NH, the preferred magnetic coupling is ferrimagnetic for the Cr cluster larger than two atoms, and the magnetic interaction in the Cr-doped

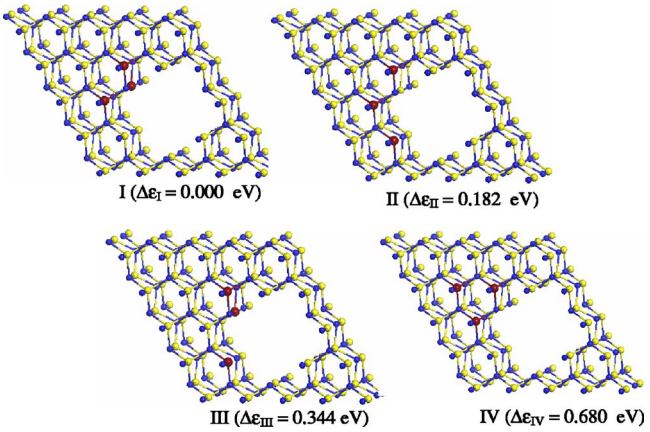

FIG. 5. (Color online) Four configurations of $Ga_{85}Cr_3N_{88}$ supercell. The lighter (yellow) spheres are Ga, the darker (blue) and smaller spheres are N, and the darker, bigger (red) spheres are Cr.

NH is shorted ranged, as found in the Cr-doped GaN bulk system.[30,31]

The transition from ferromagnetism to ferrimagnetism as the Cr cluster size increased from two to three and four Cr atoms can be understood from the Cr-Cr interatomic distances. The interatomic distance between two Cr atoms in the Cr_2-doping case is 3.102 Å and the coupling is ferromagnetic. When three Cr atoms form a cluster and occupy the sites marked (3, 2, 6) in Fig. 1, ferromagnetic coupling exists between Cr atoms on sites 3 and 2 lying at a distance of 3.105 Å. However, the Cr atom on site 6 coupled antiferromagnetically with Cr atoms at sites 2 and 3 are, respectively, at a distance of 3.013 and 2.956 Å. Note that these distances are shorter than the distance between ferromagnetically coupled Cr atoms. It has been demonstrated before that shorter distances favor antiferromagntic coupling while longer distances favor ferromagnetic coupling.[30] Similar trend also occurs when four Cr atoms occupying sites (3, 2, 7, 6) (see Fig. 1) with (down, up, up, up) spin pattern form a cluster. The interatomic distances between ferromagnetically coupled sites 2 and 7 and sites 2 and 6 are, respectively, 3.170 and 3.163 Å. On the other hand, the distance between antiferromagnetically coupled sites 3 and 2 is 3.010 Å, and the distance between sites 3 and 6 is 2.951 Å. Thus the magnetic coupling is sensitive to the distance separating the Cr atoms and the resulting magnetism will depend upon the cluster size.

To see if the underlying reason for the clustering of Cr is associated with the oxidation state of Cr (namely, is it zero?), we have calculated the charge on the Cr atom by integrating the electron charge density within the Wigner-Seitz cell. Based on this calculation, we found that the oxidation state of Cr is close to +2. However, the quantitative significance of this oxidation state has to be interpreted with caution as it very much depends upon how the charge densities are partitioned. Since there is no experimental information available on the oxidation state of Cr doped in GaN, we have compared it with Mn doped GaN where electron spin resonance (ESR) experiment[32] suggested an oxidation state of Mn to be +3. Since the Pauling electronegativity of Cr and Mn atoms are 1.66 and 1.55, respectively, one would expect that the oxidation state of Cr would be smaller than that of Mn (i.e., +3) in the similar bonding environment. Therefore +2 oxidation state for Cr seems reasonable. Thus the repulsion between two Cr^{2+} ions certainly would not lead to clustering. The clustering we have observed is mediated by the interaction between Cr 3*d* and neighboring N 2*p* orbitals. The indirect *d-d* interaction between Cr atoms is mediated by Cr-3*d* and N-2*p* hybridization. This indirect *d-d* interaction results in a lower binding energy, compared to that in the nonclustering case.

It is legitimate to ask if there is a critical size for a cluster. Note that there are two main competing factors which determine the cluster size of the dopant. The first one is the Coulomb repulsion among Cr ions, which is unfavorable for clustering and limits the cluster size. The second one is the indirect *d-d* interactions among Cr ions meditated by N, which favors clustering. As discussed above, when more Cr is doped and the cluster size increases, the AFM coupling would become stronger. Accordingly the average Cr-Cr distance would decrease, and the Coulomb repulsion will increase. Therefore the clustering tendency decreases with increasing size and doping concentration. In fact, our results suggested that the energy gain becomes less and less when going from 0 to 1, 2, 3, and 4 doped Cr atoms. Hence at some point where the Coulomb repulsion dominates, clustering would stop. We also note that doping introduces impurity states in the energy gap. The hybridized Cr-N states contribute to the impurity states, which make the system half-metallic in low doping concentration. It can be expected that doping with high concentration would improve the metallicity of the system.

IV. SUMMARY

In conclusion, we have studied the electronic and magnetic properties of Cr-doped GaN NH generated from GaN wurtzite crystalline structure, using GGA as well as GGA +U methods. We have shown that the coupling between two Cr atoms in the GaN NH is FM with each Cr atom carrying a magnetic moment of $2.786\mu_B$ and $2.129\mu_B$. The FM coupling results from the charge overlap between Cr 3*d* and N 2*p* with the N atom mediating the coupling between the two Cr atoms. As the concentration of Cr atoms increase, they have a strong tendency to cluster and couple ferrimagneticlly. Consequently, clustering leads to a small average magnetic moment per Cr atom in the NH. For example, where three (four) Ga atoms are replaced by Cr atoms, the average magnetic moment per Cr atom is found to be 0.86 $(1.62)\mu_B$, respectively. Thus the magnetic coupling of Cr atoms and their tendency to form embedded clusters in GaN are found to be independent of whether the sample is a crystal, thin film, NW, or NH. Therefore experimental synthesis conditions have to be tailored so as to prevent clustering of Cr atoms.

ACKNOWLEDGMENTS

The work was supported in part by a grant from the Office of Naval Research. The authors thank the crew of the Center for Computational Materials Science, the Institute for Materials Research, Tohoku University (Japan), for their continuous support of the HITACH SR8000 supercomputing facility.

[1] T. W. Ebbesen, H. J. Lezec, H. F. Ghaemi, T. Thio, and P. A. Wolff, Nature (London) **391**, 667 (1998).
[2] M. Law, J. Goldberger, and P. Yang, Annu. Rev. Mater. Res. **34**, 83 (2004).
[3] E. Altewischer, M. P. van Exter, and J. P. Woerdman, Nature (London) **418**, 304 (2002).
[4] W. L. Barnes, A. Dereux, and T. W. Ebbesen, Nature (London) **424**, 824 (2003).
[5] P. Andrew and W. L. Barnes, Science **306**, 1002 (2004).
[6] T. Thio, H. J. Lezec, T. W. Ebbesen, K. M. Pellerin, G. D. Lewen, A. Nahata, and R. A. Linke, Nanotechnology **13**, 429 (2002).
[7] D. Jenkins, W. Clegg, J. Windmill, S. Edmund, P. Davey, D. Newman, C. D. Wright, M. Loze, M. Armand, R. Atkinson, B. Hendren, and P. Nutter, Microsyst. Technol. **10**, 66 (2003).
[8] M. Westphalen, U. Kreibig, J. Rostalski, H. Luth, and D. Meissner, Sol. Energy Mater. Sol. Cells **61**, 97 (2000).
[9] P. M. Tessier, O. D. Velev, A. T. Kalambur, J. F. Rabolt, A. M. Lenhoff, and E. W. Kaler, J. Am. Chem. Soc. **122**, 9554 (2000).
[10] J. Homola, S. S. Yee, and G. Gauglitz, Sens. Actuators B **54**, 3 (1999).
[11] J. Liang, S.-K. Hong, N. Kouklin, R. Beresford, and J. M. Xu, Appl. Phys. Lett. **83**, 1752 (2003).
[12] Y. D. Wangand, S. J. Chua, M. S. Sander, P. Chen, S. Tripathy, and C. G. Fonstad, Appl. Phys. Lett. **85**, 816 (2004).
[13] A. P. Vajpeyi, S. Tripathy, L. S. Wang, B. C. Foo, S. J. Chua, E. A. Fitzgerald, and E. Alves, J. Appl. Phys. **99**, 104305 (2006).
[14] A. P. Vajpeyi, S. J. Chua, S. Tripathy, E. A. Fitzgerald, W. Liu, P. Chen, and L. S. Wang, Electrochem. Solid-State Lett. **8**(4), G85 (2005).
[15] N. A. Kouklin and J. Liang, J. Electron. Mater. **35**, 1133 (2006).
[16] A. P. Vajpeyi, S. Tripathy, S. R. Shannigrahi, B. C. Foo, L. S. Wang, S. J. Chua, and E. Alves, Electrochem. Solid-State Lett. **9**, G150 (2006).
[17] Q. Wang, Q. Sun, P. Jena, and Y. Kawazoe, Phys. Rev. Lett. **93**, 155501 (2004).
[18] Q. Wang, Q. Sun, and P. Jena, Phys. Rev. Lett. **95**, 167202 (2005).
[19] Q. Wang, Q. Sun, P. Jena, J. Z. Yu, R. Note, and Y. Kawazoe, Phys. Rev. B **72**, 045435 (2005).
[20] Q. Wang, Q. Sun, P. Jena, and Y. Kawazoe, Nano Lett. **5**, 1587 (2005).
[21] G. Kresse and J. Furthmüller, Phys. Rev. B **54**, 11169 (1996).
[22] G. Kresse and D. Joubert, Phys. Rev. B **59**, 1758 (1999).
[23] P. E. Blöchl, Phys. Rev. B **50**, 17953 (1994).
[24] Y. Wang and J. P. Perdew, Phys. Rev. B **44**, 13298 (1991).
[25] V. I. Anisimov, J. Zaanen, and O. K. Andersen, Phys. Rev. B **44**, 943 (1991).
[26] A. I. Liechtenstein, V. I. Anisimov, and J. Zaanen, Phys. Rev. B **52**, R5467 (1995).
[27] M. A. Korotin, V. I. Anisimov, D. I. Khomskii, and G. A. Sawatzky, Phys. Rev. Lett. **80**, 4305 (1998).
[28] T. Tsujioka, T. Mizokawa, J. Okamoto, A. Fujimori, M. Nohara, H. Takagi, K. Yamaura, and M. Takano, Phys. Rev. B **56**, R15509 (1997).
[29] H. J. Monkhorst and J. D. Pack, Phys. Rev. B **13**, 5188 (1976).
[30] X. Y. Cui, J. E. Medvedeva, B. Delley, A. J. Freeman, N. Newman, and C. Stampfl, Phys. Rev. Lett. **95**, 256404 (2005).
[31] L. Bergqvist, O. Eriksson, J. Kudrnovsky, V. Drchal, P. Korzhavyi, and I. Turek, Phys. Rev. Lett. **93**, 137202 (2004).
[32] T. Graf, J. Supercond. **16**, 83 (2003).